

Effect of smoking and alcohol on the hemoglobin concentration of blood: modeling and analysis using photonic crystal based race track ring resonator

UTTARA BISWAS¹, JAYANTA KUMAR RAKSHIT^{1,*}, KYRIAKOS E. ZOIROS²

¹*Department of Electronics & Instrumentation Engineering, National Institute of Technology Agartala, Agartala, 799046, India*

²*Lightwave Communications Research Group, Department of Electrical and Computer Engineering, Democritus University of Thrace, Xanthi, Greece*

Tobacco smoking and alcohol consumption has many adverse effects on human health and leads to many chronic diseases. The present study aims to compare the effect of smoking and alcohol consumption on the hemoglobin concentration of the blood of male and female smokers and non-smokers. It is proved from the study that the effect of smoking and alcohol consumption is more pronounced in the case of female smokers as compared to male smokers. A race track-shaped photonic crystal ring resonator is designed using a finite difference time domain (FDTD) simulation platform to conduct the study and a very high sensitivity of 950 nm/refractive index unit is obtained from the analysis.

(Received February 28, 2022; accepted August 10, 2022)

Keywords: Photonic crystal, Racetrack ring resonator, Tobacco smoking, Alcohol consumption, Hemoglobin concentration, Finite Difference Time Domain method

1. Introduction

Both tobacco and alcohol are deleterious to a well-being heart and a healthy lifestyle. Ceasing the habit of smoking and alcohol intake improves the quality of the physical, emotional, and financial life of an individual, moreover of society. Smokers and drinkers share the most similar lifestyle and behavioral patterns as smoking is the most common habit among alcohol drinkers.

Among the chief preventable causes of death, smoking is the most harmful throughout the world. According to the World Health Organization (WHO), worldwide almost eight million people die every year from tobacco use [1]. In India, 7% of all deaths are caused due to tobacco [2]. According to the published literature, it is found that India has the second-highest number of smokers [3]; around 47% of adult men and 14% of adult women in India either smoke or chew tobacco [3]. It is shown that relative risks of tobacco smoking are higher in the case of women as compared to men [4]. More than 7000 chemicals are present in cigarette smoke and smokers are exposed to many harmful substances including nicotine, carbon-mono-oxide, free radicals, etc. [5–7], that lead to cardiovascular diseases, stroke, respiratory diseases, hypertension, and also lead to cancers of the lungs, breast, and kidneys [8–13]. Moreover, smoking also affects the normal count of blood constituents [14–18]. Many research works have already been accomplished to establish the relationship between the inhalation of smoking and the total count of different blood constituents. In earlier studies, the effect of smoking on

White Blood Cells count was investigated [15, 16]. The relationship between hematological parameters and smoking has already been reported by different researchers [18, 19]. Also, the Mean Corpuscular Volume (MCV), Red Blood Cells (RBC), Mean Corpuscular Hemoglobin (MCH), and Platelets (PLT) in the blood in the case of smokers and non-smokers have been compared in earlier years [18, 19]. Cessation from smoking improves the sense of smell and taste, de-stresses the mind, improves fertility, and makes one livelier.

Smoking has also a great impact on the hemoglobin (Hb) concentration in blood [20, 21] and it causes an increase in the Hb concentration due to exposure to carbon monoxide (CO). An inactive form of Hb, carboxyhemoglobin (HbCO) is formed when Hb and CO are combined. HbCO reduces the oxygen-carrying capacity in the tissue. To maintain the oxygen level, Hb level becomes higher in smokers compared to non-smokers [22].

The habit of alcohol drinking increases the risks related to tobacco smoking. Alcohol intake risks the healthy life of an individual and leads him/her to many severe diseases, like carcinogenesis, hematological disorders, megaloblastic anemia, the disorder in intestinal absorption, and urinary excretion [23–27]. Human physiology is greatly affected by exposure to alcohol. Exposure to alcohol causes hemorheological, morphological, and biochemical modifications in RBC [23, 28, 29]. The average surface area of RBC is proved to be changed and decreased when exposed to alcohol. Abstaining from alcohol intake reduces weight and also

reduces the risks of cancer [30–32]. Excessive consumption of alcohol increases the hemoglobin concentration in the blood [33]. Also, alcohol has an increasing effect on the white blood cells count of blood [34]. The impact of tobacco smoking and alcohol consumption on the Hb concentration of blood has previously been studied in [34]. In [34] a model is formulated, designed, and analyzed using the Lumerical FDTD simulation tool [35–39] to verify the validity of the proposed scheme.

The demand for photonic crystal (PhC)-based optical technologies is rapidly growing for optical sensing applications. PhC and its applications in healthcare [40–41], refractive index (RI) sensing [42], quality control of food, and in many other fields [43–51] is now an active area of research in the present era due to the photonic band gap (PBG) property and the light confinement capability of PhC-based structures. The shifting in the resonance wavelength takes place in the two-dimensional (2D) PhC structure due to different RI of the analyte sample and changes in different environmental parameters. The sensitivity and other physical and performance parameters can be evaluated from the resonance shift in PhC.

Recently, a PhC-based Mach-Zehnder-Interferometer structure was used to detect the pressure variation using the Finite Element Method (FEM) analysis and Finite Difference Time Domain (FDTD) method, where pressure variation is calculated by measuring the shift in resonance wavelength [46].

A one-dimensional PhC structure was theoretically investigated for the detection of blood plasma and cancer cells in 2020 [47]. The detection of RI-based cancerous cells has also been proposed in the literature [49]. PhC structure containing a resonance cavity coupled with two waveguides was proposed for RI sensing purposes and investigated using FEM analysis [48].

In this paper, a PhC-based racetrack ring resonator (RTRR) is proposed for determining the Hb concentration in blood. Hb concentration in the blood is compared between smokers and non-smokers and also the effect of alcohol intake on the Hb concentration in blood is analyzed.

The paper is organized as follows: After describing the state-of-the-art and prior work in the field of optical sensors using photonic crystal technologies in section 1, section 2 describes the theoretical part of the sensor; section 3 concisely describes the proposed design; section 4 presents the simulation results; section 5 discusses different performance parameters of the sensor, and section 6 summarizes the main outcomes.

2. Theory

There is a significant relationship between the Hb concentration in the blood and the habit of smoking. From the published articles by different researchers, it is proved that smokers carry a higher concentration of Hb compared to non-smokers [29–34]. The amount of alcohol intake also plays a significant role in the Hb levels and it becomes more significant in the case of smokers. Also, women are

more vulnerable to the impact of alcohol intake on Hb levels [29].

The relationship between the Hb levels and the RI of blood has been well established by researchers [52]. As no chemical interaction occurs between the components of the multi-component biological medium (blood), the RI of blood is consequently the average of RI of its components with their volume fractions as weighting factors [53], as described in Eq. 1.

$$n_{blood} = n_e V_e + n_p n_p \quad (1)$$

where RI of erythrocytes and RI of blood plasma are indicated by n_e and n_p , respectively, while V_e and V_p stand for their volume fractions. Blood cells and platelets are present in very small amounts in the blood, so they have a negligible effect on the RI.

The RI of an erythrocyte depends on the Hb concentration present in it. A linear relationship is maintained by the RI of erythrocyte with the Hb concentrations present in the whole blood, which was described by the Gladstone-Dale equation by Ghosh *et al.* in 2006 [54]. According to the Gladstone-Dale equation,

$$n_e = n_0 + \beta * MCHC(g/dL) \quad (2)$$

where n_0 represents the RI of cell fluid in the absence of Hb, the value of which is 1.335, β is the proportionality constant having the value of 0.0019dL/g, and Mean Cell Hemoglobin Concentration is represented by MCHC.

The MCHC is the ratio of the Hb concentration in the whole blood to the volume fraction of RBC and can be described by Eq. 3.

$$MCHC(g/dL) = \frac{\text{Hb concentration in blood (g/dL)}}{\text{volume fraction of RBC}} \quad (3)$$

3. Proposed structure

RTRR has currently gained great attention from researchers for its flexibility in different applications [54–56]. PhC-based RTRR enhances this flexibility as it offers a wide range of design parameters, such as the lattice distance of the PhC structure, the radius of the scattering rods, the optical path length of the ring, and the coupling length between the straight waveguides and the ring, and so on. The longer coupling length allows more numbers of photons to be coupled through the waveguides and thus increases the quality factor of the ring. The proposed PhC-based RTRR structure is created using Si rods placed in the silica (SiO₂) slab in the form of a square-type lattice structure, as depicted in Fig. 1. The Si rods are placed in a periodic manner with a lattice distance of 540 nm and have a radius of 110 nm. The lattice constant, the rod radius, and other parameters are optimized by making first a literature survey and applying the FDTD simulation method. The PBG property of a PhC does not allow light

at a certain range of frequencies to propagate through the crystal. By creating a line defect, the periodicity of the crystal structure is broken and light is allowed to pass through the crystal. By removing two rows of the crystal structure, the propagation waveguide and the dropping waveguide are created. An elliptical row of rods is removed to create a racetrack-shaped ring resonator. To improve efficiency and give the ring the perfect racetrack shape, some inner rods of the ring are moved in the inward direction. The optimized racetrack-shaped ring contains fifteen rods along the major radius and seven rods along

the minor radius. To place the analyte sample, an elliptical-shaped rim is also etched in the silica slab. In practice, an aqueous solution of the analyte can be delivered by injection, by free-fluid flow, or by integrated microfluidic channels onto the holes which are shown in Fig. 1 [57].

The inner and outer major and minor radius of the ring and all other design parameters are optimized through numerical simulation. The optimized parameters are tabulated in Table 1.

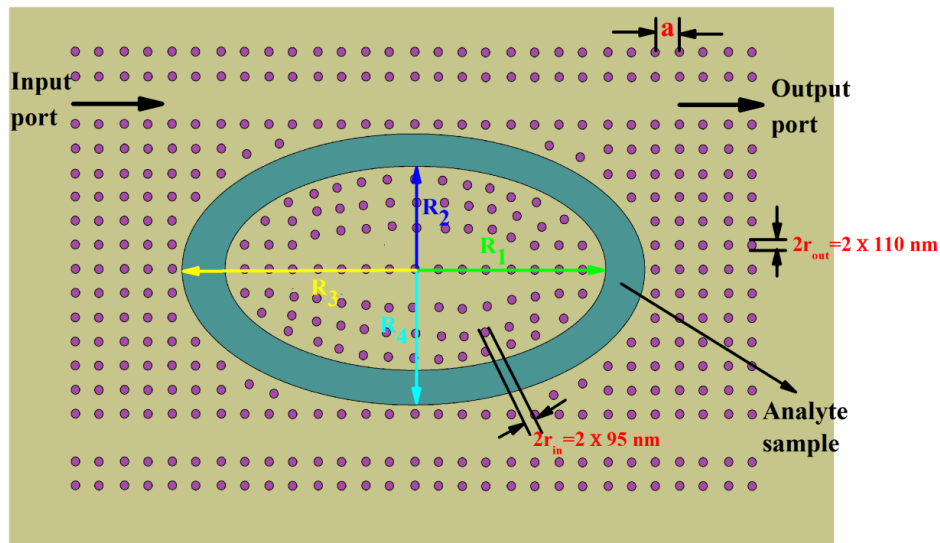


Fig. 1. Proposed design of race-track shaped ring resonator (color online)

Table 1. Design parameters of proposed RTRR

Sl. No.	Parameters	Specification
1.	Configuration	Rod-type structure
2.	Lattice architecture	Square-type lattice
3.	The radius of outer Si rods of the ring (r_{out})	110 nm
4.	The radius of the inner rods of the ring (r_{in})	95 nm
5.	Lattice distance (a)	540 nm
6.	Height of the rod	360 nm
7.	Number of rods along with X and Y directions	29×19
8.	The inner major radius of the rim (R_1)	4000 nm
9.	The inner minor radius of the rim (R_2)	2200 nm
10.	The outer major radius of the rim (R_3)	5120 nm
11.	The outer minor radius of the rim (R_4)	3120 nm
12.	Substrate material	SiO_2
13.	Footprint	Around $180 \mu\text{m}^2$

The PBG diagram of the proposed PhC structure is obtained by the plane wave expansion (PWE) method. The PBG structure for the transverse magnetic (TM) mode is depicted in Fig. 2. From the band gap diagram, it is clear that three band gaps exist for the proposed structure. Thus the input light should lie within these band gap

frequencies. The first PBG has wavelength intervals from 1309.9 nm to 1949.7 nm, which contains the transmission band known as the 'third window' and is widely exploited in modern optical communications. This wavelength range defines the range of sensing of the proposed structure.

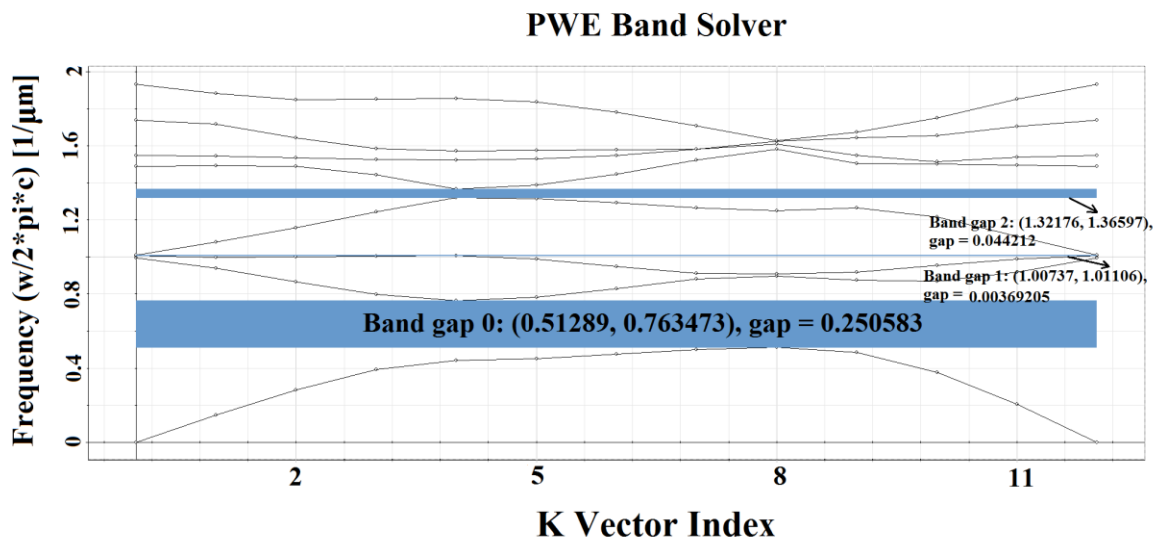


Fig. 2. PBG diagram for TM mode (color online)

4. Simulation results

Lumerical-based 2D FDTD simulation is used to simulate the proposed structure. 2D simulation is much faster and uses less memory compared to a 3D FDTD simulation. A 2D FDTD simulation in the FDTD Solution platform will simply take the cross-section of the physical structure assuming that the structure is uniform in the third dimension. The orientation of the 2D simulation region can only be z-normal and should be considered uniform and infinite along the z-direction. Therefore, the slab thickness has no impact on the simulation results in the 2D simulation method.

The employed FDTD tool is a commercial-grade simulation software included within Lumerical's DEVICE Multiphysics Simulation Suite. The FDTD method uses electromagnetics theory to simulate complex geometries, and by solving Maxwell's equations a researcher can tackle various types of problems encountered in computational photonics.

4.1. Effect of smoking on hemoglobin concentrations

In the case of men of different age groups, the Hb concentration in blood is not much affected by the habit of smoking. However, in the case of adult women, there is a gradual increase in the Hb concentration with age for tobacco smoking. For both genders, the habit of smoking leads to a higher Hb concentration in blood compared to non-smokers, and in the case of women, age is a significant parameter for smokers in terms of Hb concentration in blood. Smokers have higher Hb concentrations than non-smokers for both genders. The Hb concentration is 1.8 g/l higher in the case of smokers in the 30 to 60 years of age group of men, whereas in the case of women it is much higher as 1.9 g/l for the 30-year-old age

group of women and 5 g/l for the 50-year-old age group of women. The Hb concentration is increased by 1.2% in male smokers compared to non-smokers. But the difference in the mean Hb concentration for female smokers and non-smokers is quite high as 2.7% (1.4% for 30 years, 3.2% for 40 years, 3.7% for 50 years, and 2.3% for 60 years age group). Mean Hb concentrations for different age groups for both male and female smokers are tabulated in Table 2. The corresponding refractive indices of the blood for different Hb concentrations are also noted in Table 2. The simulation is performed for different Hb concentrations according to smoking habits in a commercial grade FDTD simulation platform. The obtained transmission characteristics for male and female smokers are depicted in Fig. 3 and Fig. 4, respectively. Fig. 4a, Fig. 4b, Fig. 4c, and Fig. 4d represent Hb concentrations for 30 years, 40 years, 50 years, and 60 years age groups of female smokers, respectively.

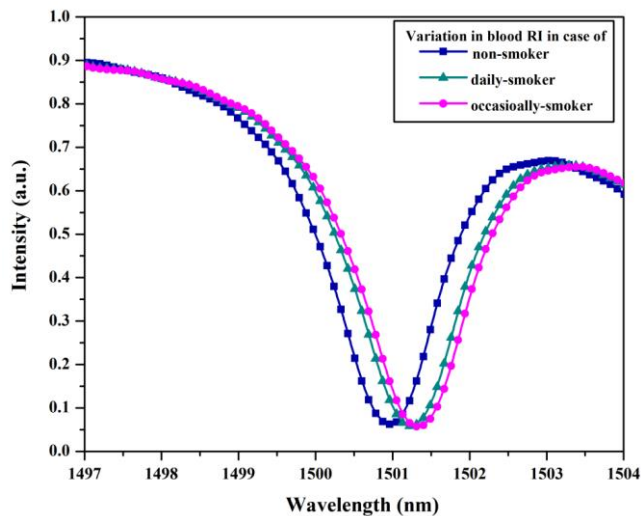


Fig. 3. Transmission graph for male smokers according to the smoking habit (color online)

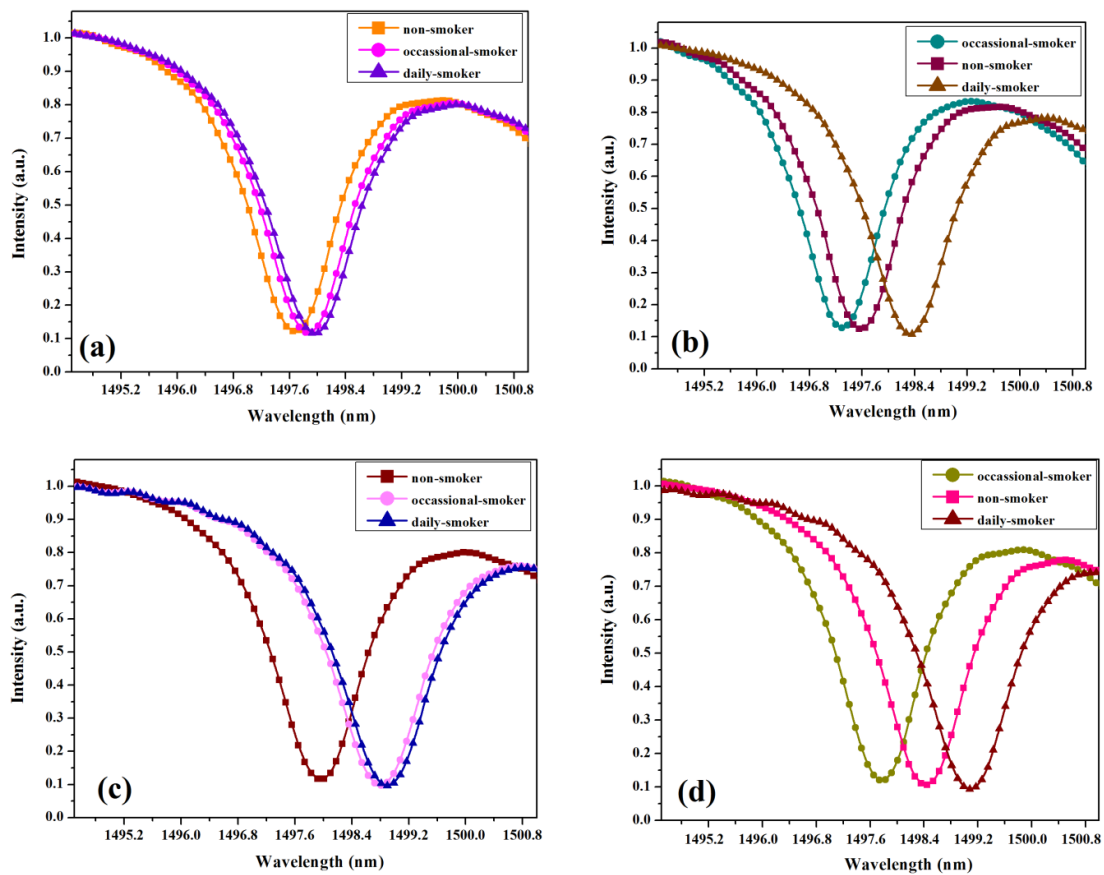


Fig. 4. Transmission graph for female smokers according to the smoking habit for (a) 30 years age groups (b) 40 years age groups (c) 50 years age groups and (d) 60 years age groups (color online)

Table 2. Hb concentrations according to smoking habits for different age groups [29]

	Smoking habit	Mean Hb concentration (g/dl)	RI of the blood	Resonance wavelength (nm)
Men Age (years) 30-60	No	15.52	1.3738	1500.98
	Occasionally	15.74	1.3742	1501.36
	Daily*	15.7	1.3741	1501.24
Women Age (years)				
30	No	13.67	1.3703	1497.64
	Occasionally	13.79	1.3705	1497.85
	Daily*	13.87	1.3706	1497.97
40	No	13.64	1.3702	1497.56
	Occasionally	13.51	1.3699	1497.29
	Daily*	14.08	1.371	1498.32
50	No	13.85	1.3706	1497.97
	Occasionally	14.33	1.3715	1498.8
	Daily*	14.36	1.3716	1498.92
60	No	14.13	1.3711	1498.45
	Occasionally	13.75	1.3704	1497.75
	Daily*	14.46	1.3718	1499.1

*Daily smokers: almost 10 cigarettes/ day

4.2. Effect of alcohol intake on hemoglobin concentrations among smokers

Alcohol consumption has a significantly increasing effect on Hb concentration in blood for daily smokers and

non-smokers. The amount of alcohol consumption is also a significant parameter for measuring the effect of alcohol intake on the hematological parameters. It is proved from studies by N. Milman and A. N. Pedersen [29] that someone who has more than 14 drinks (1 drink contains 12

gm ethanol) per week has a higher concentration of Hb than someone having less than 14 drinks per week. In the proposed scheme, someone consuming less than 14 drinks per week is considered as a light drinker, and someone consuming more than 14 drinks per week is considered as a heavy drinker. For adult men, consuming more than 14 drinks per week results in a Hb concentration 1.2% higher than consuming less than 14 drinks per week in the case of non-smokers. But for a male daily smoker, the mean Hb concentration is 1.5% higher for someone having more than 14 drinks weekly than for someone having less than 14 drinks. In the case of female non-smokers and daily smokers, the effect is much more hazardous. For a female non-smoker, the average Hb concentration is 2.1% (3.7% for the 30 years age group; 1.6% for the 40 years age group; 1% for the 50 years age group, and 2.4% for the 60 years age group) higher for light drinkers than for heavy drinkers. While female-heavy drinking daily smokers have 2.3% (3.3% for 30 years age group; 2% for 40 years age group; 1.7% for 50 years age group and 2.3% for 60 years age group) higher average percentage of Hb concentration than the light drinking daily smokers.

For male and female non-smokers and daily smokers, with the habit of light and heavy alcohol drinking, the mean Hb concentration in the blood is noted in Table 3. The RI of blood for corresponding Hb concentration and also the resonance wavelength from the FDTD

transmission graph are tabulated in Table 3. The transmission graphs obtained from the FDTD simulation for male and female non-smokers and daily smokers with the habit of light drinking and heavy drinking are shown in Fig. 5 and Fig. 6, respectively.

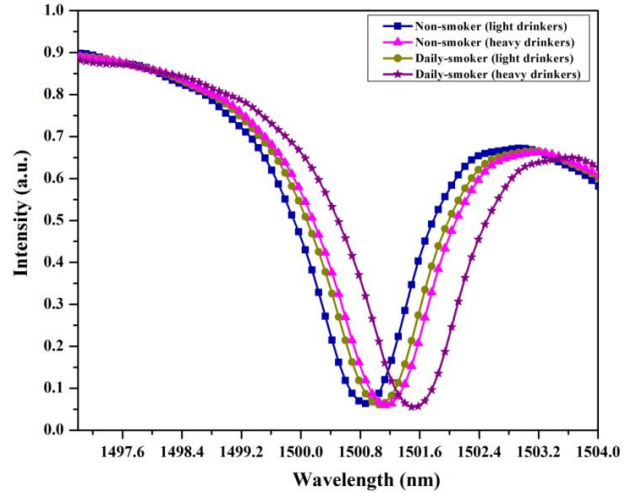


Fig. 5. Transmission graph for the effect of alcohol consumption of male smokers (color online)

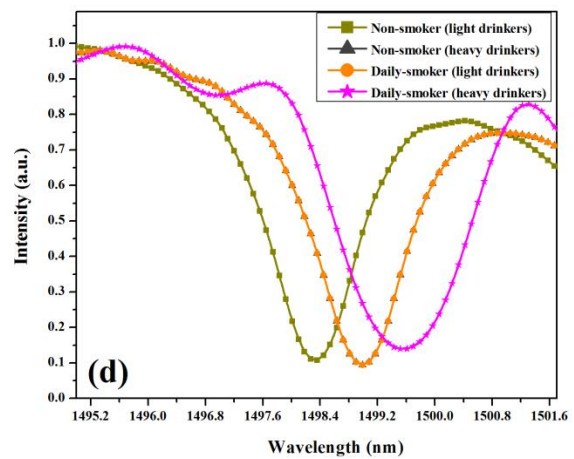
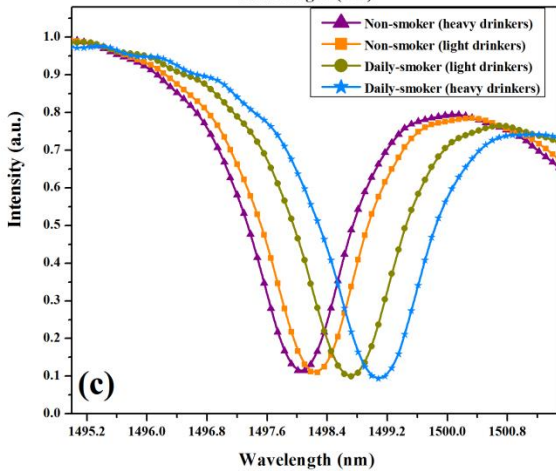
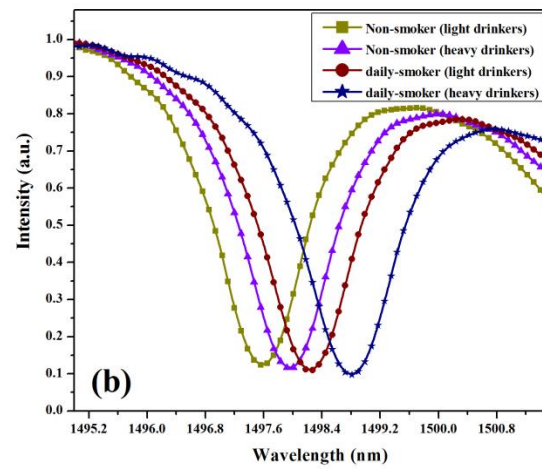
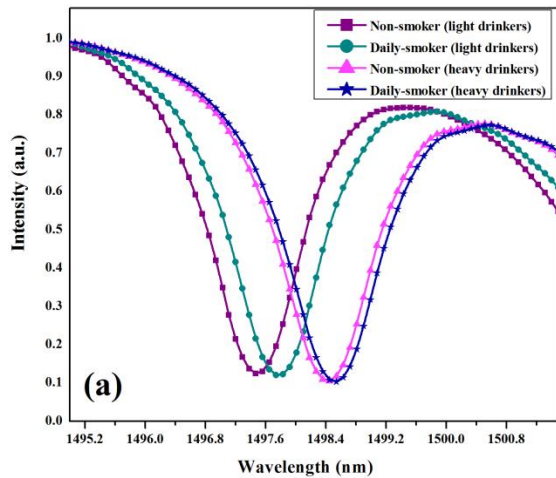


Fig. 6. Transmission graph for the effect of alcohol consumption on female smokers for (a) 30 age groups (b) 40 age groups (c) 50 age groups and (d) 60 age groups (color online)

Table 3. Effect of alcohol consumption on Hb concentrations for non-smokers and daily smokers

Gender	Smoking	Alcohol consumption #	Mean Hb concentration (g/dl)	RI of blood	Resonance wavelength (nm)
Men Age (years) 30-60	No	Light	15.47	1.3737	1500.88
	No	Heavy	15.66	1.374	1501.15
	Daily	Light	15.6	1.3739	1501.05
	Daily	Heavy	15.83	1.3744	1501.53
Women Age (years)					
30	No	Light	13.59	1.3701	1497.47
	No	Heavy	14.1	1.3711	1498.4
	Daily	Light	13.74	1.3704	1497.76
	Daily	Heavy	14.19	1.3712	1498.51
40	No	Light	13.62	1.3702	1497.59
	No	Heavy	13.84	1.3706	1497.94
	Daily	Light	14.03	1.3709	1498.22
	Daily	Heavy	14.31	1.3715	1498.81
50	No	Light	14.03	1.3709	1498.22
	No	Heavy	13.88	1.3707	1498.04
	Daily	Light	14.26	1.3714	1498.7
	Daily	Heavy	14.5	1.3718	1499.1
60	No	Light	14.06	1.371	1498.35
	No	Heavy	14.41	1.3717	1499
	Daily	Light	14.42	1.3717	1499
	Daily	Heavy	14.75	1.3723	1499.55

#Light drinkers: <14 drinks/week, Heavy drinkers: >14 drinks/week, 1 drink \cong 12 gm ethanol

5. Discussion

Due to the wide range of scalability and design parameters, PhC-based ring resonators have become very popular among researchers. Among ring resonator structures, RTRR offers a higher coupling length and thus traps more numbers of photons in the cavity. Hence RTRR has enhanced sensitivity and a higher Q factor compared to circular ring resonators [58]. The TM polarized input light passes through the propagation waveguide created by line defect; some portions of the propagating light enter the ring due to optical coupling and after multiple round-trips, light is either dropped out through the dropping waveguide or comes back to the through port. As the analyte sample has different RI places in the ring area, light interacts with different RI medium and a shift in the resonance wavelength occurs. An optical spectrum analyzer with high resolution can detect the closely related resonance wavelengths. A new generation of the high-resolution optical spectrum analyzer (BOSA from Aragon Photonics), whose combination of simultaneous high dynamic range and high resolution (0.08 pm) fits adequately our requirements for this measurement, can be considered for the proposed scheme [59-60]. The RI of the analyte for the proposed sensor can be varied from 1.36 to 1.38.

The proposed fabrication process of PhC contains mainly two steps; in the first step, a suspended organic membrane is created using direct-write EBL and in the

next step, the organic membrane is coated with silicon to create high contrast of RI [61].

For the creation of the organic membrane, at first, the substrate material is coated with a thick layer of MMA/MAA copolymer by spinning the liquid solution of the copolymer at a specific speed for a specific time. Then the structure is heated at a specific temperature to evaporate the solvent. Then again the silicon substrate is coated with a comparatively thin PMMA layer by spinning the PMMA solution and baking out the solvent at a particular temperature. Now the silicon substrate is coated with copolymer and with the PMMA layer on the top. Then the sample is exposed to EBL to pattern the PhC. As both the MAA and PMMA layers are sensitive to e-beam, the electrons can easily perforate through MAA layer, and the PMMA layer underneath the MAA layer is exposed to the e-beams and thus the polymer chains break due to the interaction with the electrons. So when the sample is immersed in the methyl isobutyl ketone (MIBK) solution, then the regions of the sample exposed to e-beam dissolve in the solution. As the MAA layer has a cessation rate higher than PMMA, it dissolves faster than PMMA as soon as holes open up in the PMMA layer. As a consequence, an expansive region of MAA is vulnerable to the MIBK solution, The PMMA is undercut and a suspended perforated membrane is created.

In EM radiation, the magnetic field is much weaker than the electric field. The force created by the electric field is much stronger than the force created by the magnetic field. So, for obtaining the intensity of light, the

electric field is preferred in the present manuscript over the magnetic field [62]. The electric field distribution of the proposed sensor for 40 years of age group of women (non-smokers and light drinkers) is given in Fig. 7.

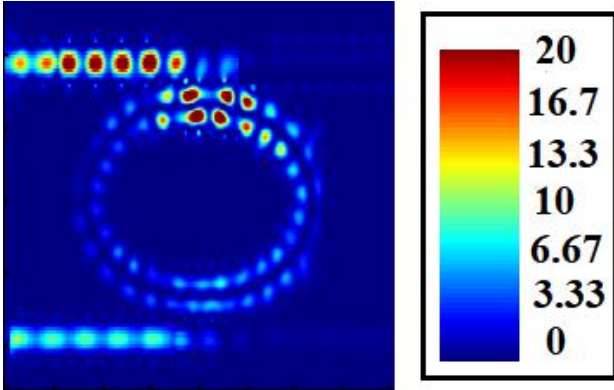


Fig. 7. Electric field distribution in the proposed sensor (color online)

The performance parameters of the proposed RTRR-based sensor are listed in the following subsections.

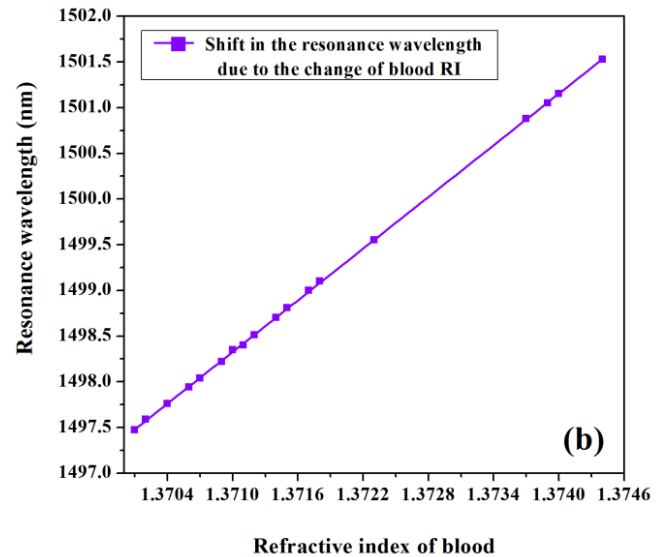
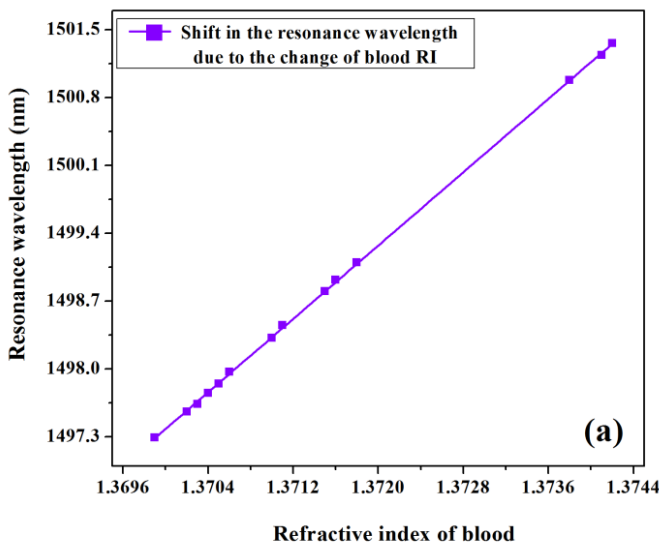


Fig. 8. Sensor sensitivity graph for (a) persons with smoking habits and (b) persons with the habit of alcohol drinking (color online)

5.2. Quality factor

The quality factor is also a significant performance parameter of a sensor. For a ring resonator-based optical sensor, the quality factor of the ring indicates the ability of the sensor to confine light within it.

5.1. Sensitivity

Sensitivity is a critical performance indicator of an optical sensor. It quantifies the ability of a sensor to detect small changes in the RI of the analyte sample. The sensitivity (S) of a sensor is expressed in terms of the shift in the resonance wavelength for the change in the RI of the analyte sample [36, 37]:

$$S = \frac{\Delta\lambda}{\Delta n} \text{ (nm/RIU)}$$

where $\Delta\lambda$ denotes the shift in the resonance wavelength and Δn stands for change in the RI of the analyte sample.

The graph of the proposed sensor sensitivity for persons with the habit of smoking and the habit of alcohol drinking is shown in Fig. 8a and Fig. 8b, respectively. The sensitivity of the proposed RTRR-based optical sensor is derived from Fig. 8 and found to be as high as 950 nm/RIU.

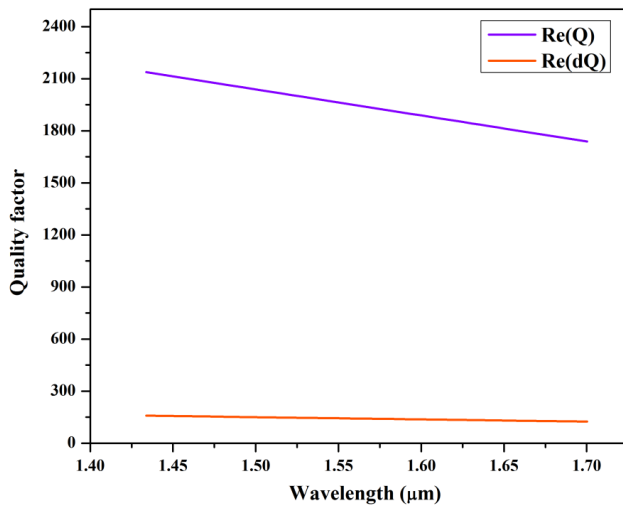


Fig. 9. Quality factors for different wavelengths (color online)

5.3. Figure of merit

The figure of merit (FOM) is expressed as the ratio of the sensitivity to the full-width half maximum (FWHM) of the resonance peak. The resonance peak has an FWHM of almost 1.8 nm. Therefore, the proposed sensor has a high FOM of about 530/RIU.

The proposed sensor exhibits high sensitivity, high-quality factor, and high FOM compared to recently published articles on PhC-based sensors [36, 48, 63]. An informative comparison between recently published articles and the proposed sensor is given in Table 4. The comparison reveals that the sensitivity of the proposed sensor outperforms by far that of the other schemes, while its other characteristics are better than the majority of these works.

Table 4. Comparison between recently published articles and the proposed sensor

Sl. No.	Authors	Sensitivity	Quality factor	FOM	Proposed structure	Application	Simulation platform
1.	U. Biswas et. al. [36]	700 nm/RIU	2500	200/RIU	PhC-based microring resonator	Detection of Hb concentration in blood	FDTD
2.	C. Qi et.al. [48]	303.65 nm/RIU	1.38×10^4	357.2/RIU	PhC-based nanocavity structure	RI sensing	FEM
3.	M. Danaie and B. Kiani [63]	720 nm/RIU and 638 nm/RIU	25-30	541.5/RIU and 471.9/RIU	PhC-based structures	RI sensor for biomedical applications	FDTD simulation and experimental work
4.	X. Qing and M. H. Sani [64]	400 nm/RIU	1080.615	258.333/RIU	Nanocavity structure based on PhC	RI sensor for detection of gases	FDTD
5.	Proposed sensor	950 nm/RIU	2000	530/RIU	PhC-based RTRR	To detect the effect of smoking and alcohol intake on the hemoglobin concentration of blood	FDTD

6. Conclusion

In summary, we deduced that tobacco smoking has a significant effect on Hb concentration in blood and has an increasing effect on both genders. However, the effect is more pronounced in women of different age groups. Likewise, an increasing effect of Hb concentration in blood with alcohol consumption is observed in the present communication and it enhances the effect in the case of smokers. An RTRR-based sensor was proposed to detect different Hb concentrations of blood for persons with the

habit of tobacco smoking and alcohol consumption. The proposed RTRR-based sensor is highly sensitive to the RI changes of the analyte sample with refractive index variation from 1.36 to 1.38 and has a sensitivity of 950 nm/RIU. The structure has also a very high Q factor of 2000 and a high FOM of 530/RIU. Owing to these attractive achievable characteristics, the proposed RTRR-based sensor can be exploited in a wide range of applications in the field of clinical practice.

References

- [1] World Health Organization. WHO report on the global tobacco epidemic, 2019: offer help to quit tobacco use (2019).
- [2] World Health Organization. Global Report on Tobacco Attributable Mortality, 2012. Geneva: WHO. (2012).
- [3] M. Rani, S. Bonu, P. Jha, S. Nguyen, L. Jamjoum, *Tobacco Control* **12**(4), e4(1-8) (2003).
- [4] A. Hackshaw, J. K. Morris, S. Boniface, J.-L. Tang, D. Milenkovic, *Bmj* **360**, j5855 (2018).
- [5] US Department of Health and Human Services. The health consequences of smoking—50 years of progress: a report of the Surgeon General (2014).
- [6] R. N. Gitte, *Asian Journal of Medical Sciences* **2**(3), 181 (2011).
- [7] R. J. Robinson, C. Yu, *Aerosol Science & Technology* **34**(2), 202 (2001).
- [8] L. E. C. Alexander, S. Shin, J. H. Hwang, *Chest* **148**(5), 1307 (2015).
- [9] J. Tredaniel, P. Boffetta, R. Saracci, A. Hirsch, *European Respiratory Journal* **7**(1), 173 (1994).
- [10] S. Baba, H. Iso, T. Mannami, S. Sasaki, K. Okada, M. Konishi, S. Tsugane, *European Journal of Preventive Cardiology* **13**(2), 207 (2006).
- [11] R. Benfante, D. Reed, J. Frank, *American Journal of Public Health* **81**(7), 897 (1991).
- [12] S. Gandini, E. Botteri, S. Iodice, M. Boniol, A. B. Lowenfels, P. Maisonneuve, P. Boyle, *International Journal of Cancer* **122**(1), 155 (2008).
- [13] P. H. Chyou, A. M. Nomura, G. N. Stemmermann, *Annals of Epidemiology* **3**(3), 211 (1993).
- [14] W. Jedrychowski, U. Maugeri, B. Adamczyk, *Giornale Italiano di Medicina del Lavoro* **8**(2), 53 (1986).
- [15] G. A. Abel, J. T. Hays, P. A. Decker, G. A. Croghan, D. J. Kuter, N. A. Rigotti, *Mayo Clinic Proceedings, Elsevier* **80**(8), 1022 (2005).
- [16] R. S. Carel, J. Eviatar, *Preventive Medicine* **14**(5), 607 (1985).
- [17] E. D. Van Tiel, P. H. Peeters, H. A. Smit, N. J. Nagelkerke, A. J. M. Van Loon, D. E. Grobbee, H. B. Bueno-De-Mesquita, *Annals of Epidemiology* **12**(6), 378 (2002).
- [18] S. Brar, *Group* **31**, 40 (2014).
- [19] M. Asif, S. Karim, Z. Umar, A. Malik, T. Ismail, A. Chaudhary, M. Hussain Alqahtani, M. Rasool, *Turkish Journal of Biochemistry/Turk Biyokimya Dergisi* **38**(1), 75 (2013).
- [20] B. Shah, A. Nepal, M. Agrawal, A. Sinha, *Sunsari Technical College Journal* **1**(1), 42 (2012).
- [21] A. Goel, D. Deepak, N. Gaur, *Journal of Pharmaceutical and Biomedical Sciences* **1**(01), 1 (2010).
- [22] R. Aitchison, N. Russell, *Journal of the Royal Society of Medicine* **81**(2), 89 (1988).
- [23] A. A. Howard, J. H. Arnsten, M. N. Gourevitch, *Annals of Internal Medicine* **140**(3), 211 (2004).
- [24] J. Potter, D. Beevers, *The Lancet* **323**(8369), 119 (1984).
- [25] K. Rasineni, M. P. Srinivasan, A. N. Balamurugan, B. S. Kaphalia, S. Wang, W. X. Ding, S. J. Pandol, A. Lugea, L. Simon, P. E. Molina, P. Gao, *Biomolecules* **10**(5), 669 (2020).
- [26] G. Corrao, V. Bagnardi, A. Zambon, C. La Vecchia, *Preventive Medicine* **38**(5), 613 (2004).
- [27] A. L. Klatsky, *Annals of the New York Academy of Sciences* **957**(1), 7 (2002).
- [28] S. Y. Lee, H. J. Park, C. Best-Popescu, S. Jang, Y. K. Park, *PloS One* **10**(12), 0145327 (2015).
- [29] N. Milman, A. N. Pedersen, *Annals of Hematology* **88**(7), 687 (2009).
- [30] D. F. Williamson, M. R. Forman, N. J. Binkin, E. M. Gentry, P. L. Remington, F. L. Trowbridge, *American Journal of Public Health* **77**(10), 1324 (1987).
- [31] P. Boffetta, M. Hashibe, *The Lancet Oncology* **7**(2), 149 (2006).
- [32] V. Bagnardi, M. Blangiardo, C. La Vecchia, G. Corrao, *British Journal of Cancer* **85**(11), 1700 (2001).
- [33] G. N. Ioannou, J. A. Dominitz, N. S. Weiss, P. J. Heagerty, K. V. Kowdley, *Gastroenterology* **126**(5), 1293 (2004).
- [34] H. Parry, S. Cohen, J. E. Schlarb, D. A. Tyrrel, A. Fisher, M. A. Russell, M. J. Jarvis, *American Journal of Clinical Pathology* **107**(1), 64 (1997).
- [35] U. Biswas, J. K. Rakshit, G. K. Bharti, *Optical and Quantum Electronics* **52**(1), article no. 19 (2020).
- [36] U. Biswas, J. K. Rakshit, *Optical and Quantum Electronics* **52**(10), article no. 449 (2020).
- [37] U. Biswas, J. K. Rakshit, M. P. Singh, 2020 International Conference on Computational Performance Evaluation (ComPE), IEEE 153 (2020).
- [38] U. Biswas, J. K. Rakshit, J. Das, G. K. Bharti, B. Suthar, A. Amphawan, M. Najjar, *Silicon* **13**, 885 (2021).
- [39] U. Biswas, J. K. Rakshit, B. Suthar, D. Kumar, C. Nayak, *International Journal of Numerical Modelling: Electronic Networks, Devices and Fields* **35**(2), 2962 (2021).
- [40] M. R. Rakhshani, M. A. Mansouri-Birjandi, *Sensors and Actuators B: Chemical* **249**, 168 (2017).
- [41] M. R. Rakhshani, *Optical and Quantum Electronics* **53**(5), 1 (2021).
- [42] M. R. Rakhshani, *IEEE Sensors Journal* **22**(5), 4043 (2022).
- [43] M. R. Rakhshani, M. A. Mansouri-Birjandi, *Plasmonics* **12**(4), 999 (2017).
- [44] M. R. Rakhshani, M. A. Mansouri-Birjandi, *IEEE Sensors Journal* **16**(9), 3041 (2016).
- [45] M. R. Rakhshani, M. Rashki, *Optics Express* **30**(7), 10387 (2022).
- [46] V. R. Kolli, I. Bahaddur, S. Talabattula, *Results in Optics* **5**, 100118 (2021).
- [47] A. Bijalwan, B. K. Singh, V. Rastogi, *Optik* **226**, 165994 (2021).
- [48] C. Qi, W. Shutao, L. Jiangtao, L. Na, P. Bo, *Optics Communications* **464**, 125393 (2020).

- [49] A. Panda, P. P. Devi, *Optical Fiber Technology* **54**, 102123 (2020).
- [50] H. Chopra, R. S. Kaler, B. Painam, *Journal of Nanophotonics* **10**(3), 036011 (2016).
- [51] V. Kaur, S. Singh, *Journal of Nanophotonics* **13**(2), 026011 (2019).
- [52] O. Zhernovaya, O. Sydoruk, V. Tuchin, A. Douplik, *Physics in Medicine & Biology* **56**(13), 4013 (2011).
- [53] E. N. Lazareva, V. V. Tuchin, *Journal of Biomedical Photonics & Engineering* **4**(1), 35 (2018).
- [54] N. Ghosh, P. Buddhiwant, A. Uppal, S. Majumder, H. Patel, P. Gupta, *Applied Physics Letters* **88**(8), 084101 (2006).
- [55] M. A. Mansouri-Birjandi, A. Tavousi, *International Journal of Natural and Engineering Sciences* **7**(1), 1 (2013).
- [56] G. Reed, W. Headley, F. Gardes, B. Timotijevic, S. Chan, G. Mashanovich, *Proc. of SPIE, Integrated Optics, Silicon Photonics, and Photonic Integrated Circuits* **6183**, 6183G (2006).
- [57] R. Arunkumar, T. Suaganya S. Robinson, *Photonic Sensors* **9**(1), 69 (2019).
- [58] N. Kazanskiy, S. N. Khonina, M. A. Butt, *Sensors* **20**(12), 3416 (2020).
- [59] A. Villafranca, J. A. Lázaro, I. Salinas, I. Garcés, *IEEE Photonics Technology Letters* **17**(11), 2268 (2005).
- [60] M. A. Quintela, R. A. Perez-Herrera, I. Canales, M. Fernandez-Vallejo, M. Lopez-Amo, J. M. López-Higuera, *IEEE Photonics Technology Letters* **22**(6), 368 (2010).
- [61] D. W. Prather, J. A. Murakowski, S. Venkataraman, Y. Peng, A. Balcha, T. Dillon, D. Pustai, *Micromachining Technology for Micro-Optics and Nano-Optics*, *Proc. SPIE* **4984**, 89 (2003).
- [62] M. Edward Purcell, David J. Morin, *Electricity and Magnetism* (3rd ed.). Cambridge: Cambridge Univ. Press (2012).
- [63] M. Danaie, B. Kiani, *Photonics and Nanostructures Fundamentals and Applications* **31**, 89 (2018).
- [64] P. Sami, M. H. Sani, H. Behzadnia, C. Shen, *Journal of Research in Science, Engineering and Technology* **8**(4), 50 (2020).

*Corresponding author: jayantarakshit.eie@nita.ac.in